Influence of Sodium Hydroxide on the Austenitic 330Cb Alloy Oxidation at High Temperature

Henri Buscail, Raphaël Rolland, Frédéric Riffard, Christophe Issartel, Cécile Combe, Pierre-François Cardey

Publication in the journal 'Oxidation of Metals' (Peer-reviewed)

Influence of Sodium Hydroxide on the Austenitic 330Cb Alloy Oxidation at High Temperature

Henri Buscail[a], Raphaël Rolland[a], Frédéric Riffard[a], Christophe Issartel[a], Cécile Combe[b], Pierre-François Cardey[b]

[a]*Université Clermont Auvergne - LVEEM, 8 rue J.B. Fabre, CS 10219, 43009 Le Puy en Velay, France*

[b]*CETIM, 7 rue de la Presse, 42952 Saint-Etienne, France*

henri.buscail@udamail.fr; raph43@hotmail.fr; frederic.riffard@udamail.fr; christophe. issartel@udamail.fr; cecile.combe@cetim.fr; pierre-francois.cardey@cetim.fr

Abstract. Sodium hydroxide is found on metallic conveyor belts as residue of the degreasing process of metallic screws put inside heat treatment furnaces at 900 °C. The 330Cb (Fe-34Ni-23Cr-1Nb-1.55Si) alloy is used to build these conveyor belts. With time, the amount of sodium hydroxide increases on the 330Cb steel surface. The aim of this work is to show the influence of the NaOH amount on the 330Cb oxidation during 48 h, at 900 °C. Results show that, on this austenitic steel, a protective silica scale formation is promoted by low oxygen containing gaseous environments and the high alloy silicon content. With low NaOH deposits the oxide layer is adherent and a SiO_2 cristobalite subscale is formed. It is also demonstrated that sodium combines with niobium to form $NaNbO_3$. When the NaOH amount exceeds 0.265 $mg.cm^{-2}$ on the alloy surface, severe oxidation is observed leading to a fast growing $FeCr_2O_4$ oxide scale.

Keywords: NaOH, 330CB Alloy, SiO_2, Cristobalite.

INTRODUCTION

The 330Cb alloy (Fe-34Ni-23Cr-1Nb-1.55Si) is generally used in high temperature carburising and nitriding conditions. These environments induce severe degradation of the conveyor unit due to a rapid weakening of the alloy. To improve the alloy carburization resistance it is assumed that the presence of an adherent oxide scale acts as a carbon and nitrogen diffusion barrier. A previous study has shown that in the 800 - 1000 °C temperature range, the 330Cb oxidation leads to a chromia scale acting as a good diffusion barrier under isothermal conditions [1]. The external manganese chromite subscale can limit the chromia scale evaporation at temperatures higher than 1000 °C [2]. Nevertheless, after cooling to room temperature, important oxide scale spallation occurred [1]. Gleeson demonstrated the significant effects of alloy composition on long-term, cyclic-oxidation resistance. Each of the alloys exhibited scale spallation; however, the manner by which spallation occurred varied between the alloys [3]. In the literature, a Fe-35Ni-18Cr-2Si alloy has been studied at high temperature [4]. It has been shown that a Cr_2O_3 scale is protective at high temperature. Nevertheless, Stevens has indicated that at temperatures higher than 1100 °C the chromium oxide CrO_3 evaporation occurs. Then, chromium depletion is observed in the oxide scale and in the alloy. On the basis of changes in the chemical

composition of the oxide film, together with spalling, the failure of heating-element wire by the development of hot spots can be explained. At failure both long-term (low temperature < 1000 °C) and shorter-term tests (temperature > 1000 °C) were found to have oxidised to the same depth. This can be explained on the basis of a depletion of chromium, which occurred at the oxide-alloy interface, and becomes insufficient for a healing process. Gleeson's work stated that the HR-160 alloy exhibited complete spallation owing largely to its relatively high silicon content (2.75 wt.%) [3]. However, the silicon was also beneficial in promoting protective scale formation when the exposed alloy was subsequently oxidised. The HR-120 alloy showed the poorest cyclic-oxidation resistance, due to poor scale adhesion and the tendency of iron (33 wt.%) to oxidise. All of the alloys underwent internal oxidation and void formation. In most cases, the extent of internal attack was significantly greater than that of metal loss. Former studies have shown that the oxidation of the 330Cb alloy at 900 °C in air lead to a poorly adherent chromia scale and did not permit a continuous silica scale formation even though the alloy contains about 2 wt.% silicon [5-7]. Then, the protection against corrosive environments is not ensured. One way to act on the oxide scale formation consists of modifying the gaseous environment, using inert gases [8]. Previous works have shown the effect of sodium salts coating on the high-temperature oxidation of alloys. Sodium chloride and sodium sulphate induce accelerated oxidation of chromium and hot corrosion processes [9-10]. Sodium carbonate coated Nickel-base alloys oxidised in air at 900 °C also show fluxing reactions but the morphology of the scales show less perturbation compared to sodium sulphates, sodium chlorides or sodium nitrates [11].

In this work, chlorine is not present and we consider the presence of sodium hydroxide on metallic conveyor belts as residue of the degreasing process of metallic pieces put inside heat treatment furnaces at 900 °C. The 330Cb alloy is often used to build these conveyor belts. With time, the amount of sodium hydroxide can increase on the 330Cb alloy surface due to residue accumulation. Based on what is known about the oxidation behaviour of this alloy, this work will focus on the influence of sodium hydroxide coatings on the 330Cb oxidation during 48 h, at 900 °C. The low oxygen potential gaseous environment used, N_2-5vol.% H_2, simulates industrial conditions in the heat treatment furnaces. In order to explain the influence of NaOH on the 330Cb oxidation, we will examine the effect of various NaOH coatings on the 330Cb alloy oxidation at 900 °C.

EXPERIMENTAL PROCEDURES

The 330Cb alloy is an austenitic stainless steel. Its composition, in weight %, is given in Table 1. 1.5 mm thick cylindrical specimens of 12 mm diameter were abraded up to the 320-grit SiC paper, then degreased with ethanol and finally dried. All oxidation tests were performed at 900 °C.

TABLE 1. Alloy composition (weight %).

Wt. %	Fe	Ni	Cr	Si	Nb	Mn	C	P	S
330Cb	Bal.	34.41	22.87	1.55	0.97	0.72	0.05	0.012	0.002

High temperature oxidation was performed during 48 h in flowing (8 l/h) nitrogen containing 5 vol.% hydrogen (N_2-5vol.% H_2). The residual pO_2 = 15 ppmv contained in the gas was measured by an oxygen analyser (Elcowa GPR 1200MS). The oxide characterisation was realised by X-ray diffraction (XRD). XRD patterns were obtained by use of a Philips X'pert MPD diffractometer (copper radiation, λk_α = 0.15406 nm). The XRD conditions were 2Θ scan, step 0.05° ranging from 10 to 80°, 8 s counting time. The oxide scale surface and cross-section morphologies have been observed in a JEOL 7600 scanning electron microscope (SEM) coupled with a LINK energy dispersive X-ray spectroscopy (EDXS). The EDXS point analyses were performed with an electron probe focused to a 1 µm spot. The sodium-hydroxide coatings were realised by using: 0.01; 0.1 and 0.3 mol.l^{-1} solutions. Immediately after dipping in the solution, the specimens were dried in warm flowing air at 40°C during 5 min. After coating, the specimens were weighted in order to determine the deposit weight per unit area. It corresponds respectively to: 7.10^{-3}; 6.8 10^{-2}; 0.262 mg.cm^{-2}. After drying, the coating was characterized by XRD and it was found that sodium hydroxide reacts with ambient carbon dioxide present in the air to form sodium carbonate Na_2CO_3 (ICDD 18-1208). During oxidation, Na_2CO_3 decomposes at 856 °C to

form Na_2O and this compound is reacting with the alloy at 900 °C. XRD patterns obtained on blank specimens before oxidation only show the presence of the autenitic structure (ICDD 03-1209). XRD results also indicate that no niobium containing intermetallics such as Nb_3Ni_2Si (ICDD 17-0097) could be detected on the alloy surface before oxidation.

RESULTS

On Figure 1, X-ray diffraction patterns obtained on blank 330Cb specimens oxidised for 48 h, in N_2-5 vol.% H_2 at 900 °C indicate that after oxidation the scale is composed of $Mn_{1.5}Cr_{1.5}O_4$ (ICDD 33-0892) and Cr_2O_3 (ICDD 38-1479). The intermetallic Nb_3Ni_2Si (ICDD 17-0097) is also detected after 48 h oxidation. This phase was not present on the alloy before oxidation and its presence is due to the silicon enrichment of the niobium nodules at high temperature. XRD patterns also show that, on the 7.10^{-3} mg.cm^{-2} coated specimen the oxide scale is composed of $Mn_{1.5}Cr_{1.5}O_4$ (ICDD 33-0892) and Cr_2O_3 (ICDD 38-1479). SiO_2 cristobalite (ICDD 39-1425) is also well detected on the specimen surface. The intermetallic Nb_3Ni_2Si (ICDD 17-0097) is not detected. On the $6.8.10^{-2}$ mg.cm^{-2} coated specimen the oxide scale is composed of $Mn_{1.5}Cr_{1.5}O_4$ (ICDD 33-0892) and a higher amount of Cr_2O_3 (ICDD 38-1479) is present on the surface. SiO_2 cristobalite (ICDD 39-1425) is present in lower concentration on the specimen surface compared to the previous one. On the 0.265 mg.cm^{-2} coated specimen, iron combines with chromium to form $FeCr_2O_4$ (ICDD 34-0140). The proportion of Cr_2O_3 (ICDD 38-1479) is low and sodium is found combined with niobium in a mixed oxide $NaNbO_3$ (ICDD 38-0846).

The scale cross-section morphology of the blank specimen oxidised in N_2-5vol.% H_2 during 48 h show that a 1 µm thick oxide scale is present. Silicon is found associated with niobium inside the alloy and no silica layer is observed at the alloy/oxide interface. The scale cross-section morphology of the 7 10^{-3} mg.cm^{-2} coated specimen oxidised in N_2-5vol.% H_2 during 48 h is shown on Figure 2. The scale is mainly composed of a 2 µm thick manganese chromite scale. EDXS analysis shows that a continuous cristobalite scale is formed at the alloy/oxide interface. The sodium amount is too low to permit its detection in the scale.

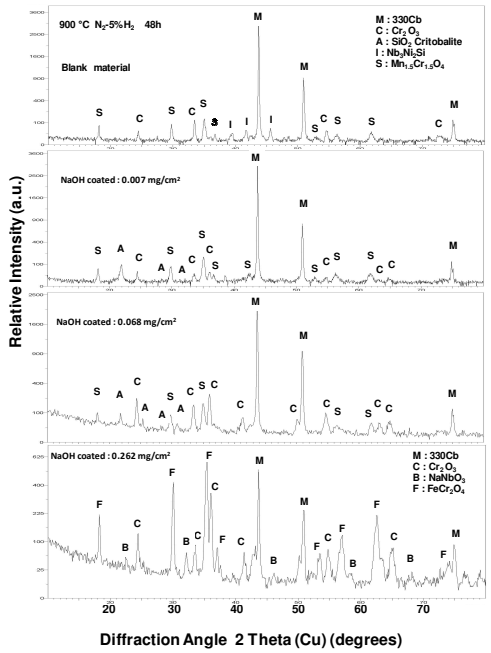

FIGURE 1. XRD patterns obtained on the 330Cb alloy after 48 h oxidation at 900°C, in N_2-5%H_2. Oxides formed on the blank material, specimens coated with 0.007 mg.cm^{-2}, 0.068 mg.cm^{-2} and 0.262 mg.cm^{-2} NaOH.

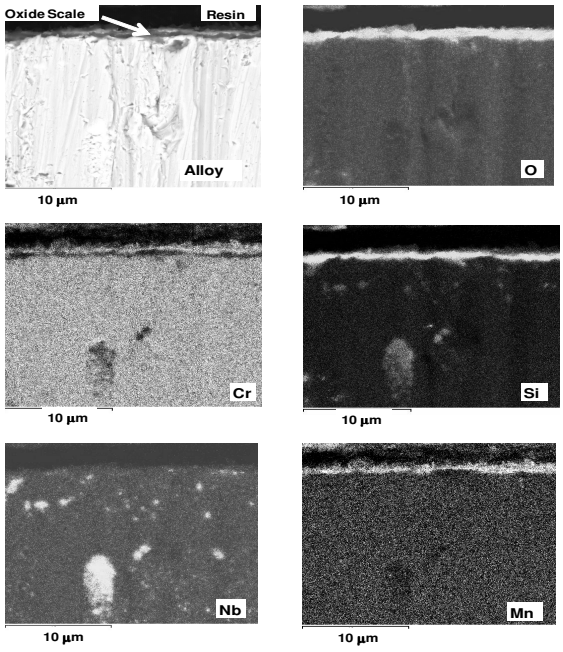

FIGURE 2. SEM cross sections obtained on the NaOH coated 330Cb specimen (7 10^{-3} mg.cm^{-2}) oxidized 48 h at 900 °C in N_2-5vol.% H_2 (BSE Image x 5000).

The scale cross-section morphology of the 6.8 10^{-2} mg.cm^{-2} coated specimen oxidised in N_2-5vol.% H_2 during 48 h is presented on Figure 3. After 48 hours oxidation at 900 °C in N_2-5vol.% H_2 the cross-section micrograph shows that the scale is mainly composed of a 4 µm thick oxide scale. EDXS analysis shows that sodium and niobium are present together in the oxide scale indicating that sodium reacts with niobium provided by the alloy. A cristobalite layer is observed on the cross section.

The scale cross-section morphology of the 0.265 mg.cm^{-2} coated specimen oxidised in N_2-5vol.% H_2 during 48 h is exhibited on Figure 4. The scale is mainly composed of a 6 µm thick iron chromite $FeCr_2O_4$ scale. Chromium depletion is observed 10 µm deep inside the alloy. Sodium and niobium are present together in the oxide scale as a $NaNbO_3$ mixed oxide identified by XRD.

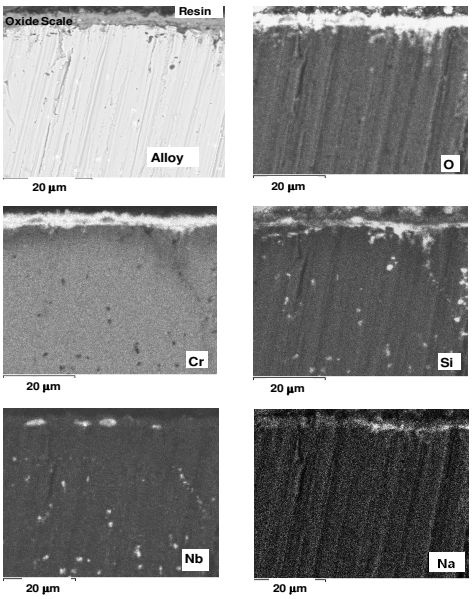

FIGURE 3. SEM cross sections obtained on the NaOH coated 330Cb specimen (6.8 10^{-2} mg.cm^{-2}) oxidized 48 h at 900 °C in N_2-5vol.% H_2 (BSE Image x 2000).

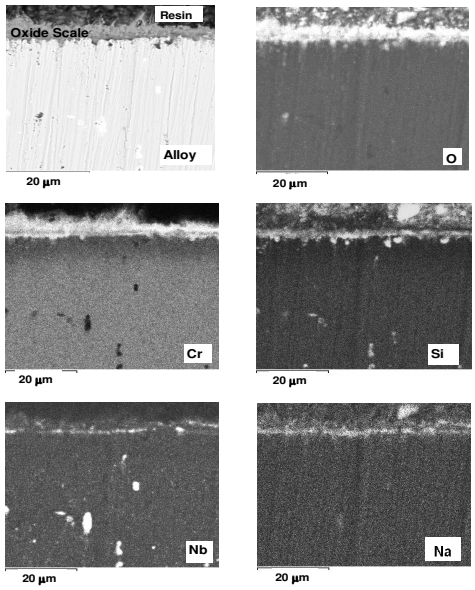

FIGURE 4. SEM cross sections obtained on the NaOH coated 330Cb specimen (0.265 mg.cm^{-2}) oxidized 48 h at 900 °C in N_2-5vol.% H_2 (BSE Image x2000).

DISCUSSION

Results show that during the 330Cb oxidation at 900 °C in N_2-5vol.% H_2 , the 15 vol.ppm oxygen partial pressure allows the chromium oxidation. This oxygen content is high enough to induce the substrate oxidation because thermodynamic data indicate that $p(O_2)=10^{-22}$ atmosphere is sufficient to oxidised chromium at 900 °C.

Thermodynamic data also indicate that $p(O_2)=10^{-30}$ atm. is enough to oxidised silicon at 900 °C. XRD results have shown that at 900 °C the oxide scales are composed of $Mn_{1.5}Cr_{1.5}O_4$ and Cr_2O_3. The relatively high $Mn_{1.5}Cr_{1.5}O_4$ peaks intensities indicate that this phase is present at the external interface. Our results show that manganese diffuses to the scale external interface in all cases. This phenomenon was reported by other authors [12-14]. $Mn_{1.5}Cr_{1.5}O_4$ is sometimes considered as non-protective because it presents a porous structure [13, 15]. Other authors pointed out that $Mn_{1.5}Cr_{1.5}O_4$ located at the external interface, could reduce the conversion of Cr_2O_3 into a CrO_3 volatile oxide above 1000 °C [16-18].

XRD and SEM results indicate that after oxidation of the blank specimen, the scale is composed of $Mn_{1.5}Cr_{1.5}O_4$ and Cr_2O_3 and no SiO_2 scale is formed after 48 h. After oxidation of 7.10^{-3} and 6.8 10^{-2} mg.cm^{-2} NaOH coated specimens, the scale is composed of Cr_2O_3 and $Mn_{1.5}Cr_{1.5}O_4$. Then, cristobalite is easily detected by XRD. EDXS analysis shows that a silica scale is present at the alloy/oxide interface (Figure 2 and Figure 3). Our results show that the silica scale formation is promoted by low oxygen containing gaseous environments such as N_2-5vol.% H_2 as demonstrated in a previous work [8]. The effect of silicon on the oxidation process has already been examined on chromia forming alloys. It generally acts as a protective element. Even though too much silicon is considered as detrimental for the steels mechanical properties [19], its addition generally

improves the oxidation resistance. Some authors stated that silicon segregates at the oxide/alloy interface and blocks the iron cationic diffusion [20-22]. Silicon is then supposed to be present as a silica film, which lowers the steel oxidation rate. The high silicon oxygen affinity permits its internal oxidation, developing SiO_2 precipitates at the internal interface [13, 23]. Then, it is reported that silica acts as a diffusion barrier and also leads to the keying of the chromia scale to the substrate [24, 25]. Silica will also lower the porosity at the internal interface acting as vacancies sinks [26]. Silicon reduces the amount of non-protective iron oxides inside the scale [27] and hinders the iron rich nodule formation [21]. It has been proposed that during the oxidation of a AISI 304 stainless steel between 900 et 1000 °C, a maximum 0.88 % (weight %) silicon content leads to the formation of a chromia scale, even at 1000 °C [28]. Nevertheless, it appears that high silicon content induces more scale spallation between the alloy and the silica scale or at the silica/chromia interface [22]. It is the reason why silicon is rarely added at more than 1 weight %. One should also take care that the chromium presence is necessary to avoid the fayalite Fe_2SiO_4 formation, which acts as a very poor diffusion barrier [29]. According to Stott, the necessary amount of silicon needed to the SiO_2 formation can be lower when the chromium content increases [29]. Concerning the effect of higher silicon additions, Li and Gleeson compared the oxidation behaviour at 1000 °C of Ni-based alloys with and without about 2.7 wt. % Si additions [30]. From oxidation results of the cast model alloys, Si addition was found to improve oxidation resistance by forming a continuous SiO_2 layer at the alloy/scale interface, which resulted in decreased oxidation kinetics. The cast alloys, with silicon addition, also showed larger average effective inter-diffusion coefficients of chromium compared to the cast alloys without silicon addition. As a consequence, the silicon addition assisted in the establishment and re-formation of a chromia scale during oxidation. In the case of commercial alloys a discontinuous distribution of SiO_2 precipitates in the vicinity of the alloy/scale interface was found to be beneficial to cyclic oxidation resistance. The formation of an amorphous silica inner layer was effective in reducing the oxidation rate of a Fe-9%Cr alloy to about half that of Si-free steel (0.06%Si) at 700 °C, in steam, when alloyed with 0.5% Si. But the effect of silicon is less beneficial at lower temperatures (500 °C) [31]. Ishitsuda et al. carried out a detailed study on the effect of Si additions between 0.06% and 0.49% on the 9Cr steel in the temperature range 500 °C-700 °C in high pressure (35 MPa) steam, and concluded that silicon was most effective in reducing the oxidation rate at the highest temperature tested and at the highest silicon content, where rates were reduced to 50% of that observed with the low silicon alloy [32]. As with the work of Ueda et al. the establishment of a complete silica layer was responsible for the protective behaviour at high test temperatures [33, 34].

In the present work, the alloy silicon content is 1.55 wt.%. Before oxidation, niobium nodules are present in the alloy and silicon is randomly distributed in the steel matrix. After oxidation of blank specimens EDXS results show that silicon is present in non-oxidised nodules at the scale/alloy interface and inside the alloy. Then, silicon is associated with niobium and nickel in the Nb_3Ni_2Si phase identified by XRD and no silica is formed.

The niobium content is 0.97 wt.% in the 330Cb alloy and should be taken into account. It is mentioned in the literature that, on austenitic steels (oxidised at 950 °C, 100h), niobium can favour the chromium diffusion in the metallic substrate to the steel/scale interface [35]. It has also been shown that the steel structures are more stable when niobium is associated with titanium and molybdenum [36]. Our results show the presence of Nb_3Ni_2Si nodules after oxidation of blank specimens. These nodules are sometimes close to the substrate surface and are not oxidised. The presence of such nodules can be explained by the fact that niobium only stays in solid solution in the alloy for temperature lower than 500 °C but not at higher temperatures [37, 38]. Our results also show that when silicon is associated with niobium in Nb_3Ni_2Si intermetallic, niobium traps silicon during oxidation and hinders the silica scale formation.

On the other hand, XRD results indicate that silicon has been oxidised and cristobalite is present on sodium hydroxide coated specimens. SEM cross sections also indicate that silicon has diffused from the substrate to permit the formation of a silica scale located at the oxide/alloy interface (Figure 1 and Figure 2). The effect of a low oxygen environment, at the alloy surface, can be related to other works describing the effect of surface coatings limiting the oxygen access to the alloy surface [8]. Some authors have shown that an yttrium sol-gel coating promotes a continuous silica scale formation at the internal interface on the alloy AISI 304 due to a limited access of the oxygen to the metallic surface [39]. Then, silica hinders the iron oxidation and the formation of non-protective iron oxides [40]. Even though the alloy 330Cb contains 1.55 wt.% silicon, results show that no continuous silica scale formation was observed after oxidation in air, at 900 °C. Some scale spallation, observed on uncoated specimens, has also been explained by the presence of the high silicon amount in the alloy [41]. The absence of iron oxides in the scale can also be due to the fact that the alloy 330Cb is a

nickel-rich alloy. Douglass [42] studied the Ni-2.05Si and Ni-4.45Si oxidation in oxygen for 18 hr in the temperature range 600-1000 °C. He proposed that the low silicon content alloy exhibited extensive internal oxidation and that the higher-silicon alloy formed a continuous layer of silicon-rich oxide. Nakakubo worked on Fe-Si and Fe-Cr alloys at 850 °C. This author calculated the boundary conditions between internal and external oxidation on the basis of the kinetic theory of the internal oxidation [43]. Onishi has also calculated the conditions at the boundary between internal to external oxidation of Si containing steels (Fe-Si alloys) at 850 °C [44]. This author has demonstrated that under low oxygen potential a very thin SiO_2 layer forms on the alloy surface because the diffusion rate of silicon is relatively high compared with that of oxygen. It is then concluded that internal oxidation occurs in a restricted oxygen partial pressure range and is limited to silicon concentrations below 1 wt.%. The oxygen partial pressure range, in which internal oxidation can occur, decreases with increasing silicon content. When the silicon content increases, external silicon oxidation should occur. In the present work, it is observed that under low oxygen potentials, the high silicon concentration in the 330Cb alloy permits the initial formation of a cristobalite scale on the alloys surface because the diffusion rate of silicon is relatively high compared with that of oxygen.

On 330Cb coated specimens, the coating was characterized by XRD and it was found that sodium hydroxide reacts with carbon dioxide to form sodium carbonate Na_2CO_3 (ICDD 18-1208). Na_2CO_3 decomposes at 856 °C to form Na_2O and this compound is the one expected to react with the alloy at 900 °C. Results shown on figure 2 and figure 3 indicate that after oxidation of 7.10^{-3} and 6.8 10^{-2} $mg.cm^{-2}$ coated specimens, a SiO_2 cristobalite scale is formed. XRD patterns show that when sodium hydroxide is deposited on the initial surface a large amount of $NaNbO_3$ phase could be detected in the oxide scale owing to its high amount (Figure 1). It should be remembered that when a crystalline phase is less present than 10 wt.%, it is hardly detected by XRD. SEM cross section (Figure 4) also shows that niobium and sodium are located at the same place. Due to the fact that the gaseous environment is always the same in this work, it is clear that sodium promotes the formation of cristobalite when low amounts of coatings are present (7.10^{-3} and 6.8 10^{-2} $mg.cm^{-2}$). Results also indicate that no intermetallic Nb_3Ni_2Si could be detected by XRD after oxidation even though the alloy is still analysed. Moreover, XRD patterns shown on Figure 1 indicate that sodium reacts with niobium to form $NaNbO_3$.

The $NaNbO_3$ formation leads to niobium depletion in the first 10 microns deep inside the alloy and not enough niobium is present to trap silicon in the Nb_3Ni_2Si intermetallic form. As a result, silicon is free to diffuse from the alloy matrix to the oxide/metal interface to form a silica scale as shown on figure 5. Results also indicate that low amounts of sodium hydroxide promote the silica crystallisation as proposed by other authors [45, 46]. The cristobalite scale then acts as a good diffusion barrier against outward iron and chromium [40]. When a very well established cristobalite scale is built, a thin adherent oxide scale is formed and mainly composed of manganese chromite. The good oxide scale adherence is then related to the direct contact between SiO_2 cristobalite and manganese chromite and their similar dilatation coefficients, respectively 7 10^{-6} K^{-1} and 7.5 10^{-6} K^{-1}. When sodium hydroxide coatings exceed 0.265 $mg.cm^{-2}$, no cristobalite protective scale forms and iron combines with chromium to form $FeCr_2O_4$. As proposed by other authors high amounts of sodium salts can induce accelerated oxidation and hot corrosion processes [9-11]. It is then concluded that if low sodium additions are beneficial for the oxidation protection of the 330Cb alloy it should not exceed 6.8 10^{-2} $mg.cm^{-2}$ on the metallic surface.

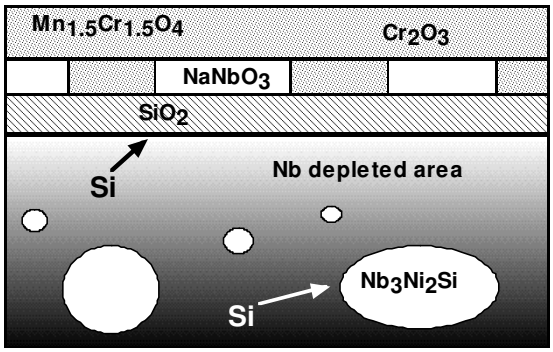

FIGURE 5. Schematic drawing showing the role of sodium-niobium interaction on the SiO_2 scale formation.

CONCLUSION

This work shows the influence of sodium hydroxide coatings on the austenitic 330Cb (Fe-34Ni-23Cr-1Nb-1.55Si) oxidation during 48 h, at 900 °C. The N_2-5vol.% H_2 gaseous environment was used in order to simulate industrial heat treatment conditions. With low NaOH deposits, the oxide scale is adherent and a SiO_2 cristobalite subscale is formed at the alloy/oxide interface. It is demonstrated that sodium combines with niobium to form $NaNbO_3$. As a niobium depleted area is formed in the alloy, results show that Nb_3Ni_2Si cannot be formed close to the internal interface and silicon is free to diffuse and oxidised as a silica scale at the oxide/alloy interface. On this austenitic steel, the protective silica scale formation is promoted by low oxygen partial pressures and the high silicon content. As the NaOH coating amount increases on the alloy surface, no protective silica scale is formed and severe oxidation is observed leading to fast growing $FeCr_2O_4$ oxide scales. To avoid any catastrophic oxidation, the maximum amount of NaOH allowed on the alloy surface is about 6.8 10^{-2} $mg.cm^{-2}$.

REFERENCES

1. H. Buscail, C. Issartel, C.T. Nguyen and A. Fleurentin, *Traitement Thermique* **394**, 31 (2009).
2. G.R. Holcomb and D.E. Alman, *Scripta Materialia* **54**, 1821 (2006).
3. B. Gleeson and M.A. Harper, *Oxidation of Metals* **49**, 373 (1998).
4. R. Stevens, *Oxidation of Metals* **13**, 353 (1979).
5. C. Issartel, H. Buscail, C.T. Nguyen and A. Fleurentin, *Materials and Corrosion* **61**, 929 (2010).
6. H. Buscail, C. Issartel, F. Riffard, R. Rolland, S. Perrier, A. Fleurentin and C. Josse, *Applied Surface Science* **258**, 678 (2011).
7. H. Buscail, C. Issartel, C.T. Nguyen, S. Perrier and A. Fleurentin, *Matériaux et Techniques* **98**, 209 (2010).
8. H. Buscail, C. Issartel, F. Riffard, R. Rolland, S. Perrier and A. Fleurentin, *Corrosion Science*, **65**, 535 (2012).
9. L. Couture, F. Ropital, F. Grosjean, J. Kittel, V. Parry and Y. Wouters, *Corrosion Science,* **55,** 133 (2012).
10. B.P. Mohanty, D.A. Shores, *Corrosion Science* **46**, 2893 (2004).
11. M. Misbahul Amin, *Thin Solid Films*, **299**, 1 (1997).
12. H.B. Grübmeier, A. Naoumidis and H.A. Schulz, *Journal of Vacuum Science and Technology* **A4**, 2565 (1986).
13. M. Landkof, A.V. Levy, D.H. Boone, R. Gray and E. Yaniv, *Corrosion Science* **41**, 344 (1985).
14. I. Saeki, T. Saito, R. Furuichi, H. Konno, T. Nakamura, K. Mabuchi and M. Itoh, *Corrosion Science* **40**, 1295 (1998).
15. N. Hussain, K.A. Shahid, I.H. Khan and S. Rahman, *Oxidation of Metals* **43**, 363 (1995).
16. C.S Tedmon, *Journal of the Electrochemical Society* **113**, 766 (1966).
17. G. Ben Abderrazik, G. Moulin and A.M. Huntz, *Oxidation of Metals* **33**, 191 (1990).
18. H.M. Tawancy, *Oxidation of Metals* **45**, 323 (1996).
19. F. Armanet, J.H. Davidson and P. Lacombe in *Les aciers inoxydables,* edited by B. Baroux, G. Beranger, Les Editions de Physique, Les Ulis France, 1990, pp. 449-489.
20. A.M. Huntz, *Materials Science and Engineering* **A201**, 211 (1995).
21. S.N. Basu and G.J. Yurek, *Oxidation of Metals* **36**, 281 (1991).
22. H.E. Evans, D.A. Hilton, R.A. Holm and S.J. Webster, *Oxidation of Metals* **19**, 1 (1983).

23. G. Aguilar, J.P. Larpin and J.C. Colson, *Mémoires et Etudes Scientifiques-Revue de Métallurgie*, 447 (1992).
24. S. Seal, S.K. Bose and S.K. Roy, *Oxidation of Metals* **41**, 139 (1994).
25. R.N. Durham, B. Gleeson and D.J. Young, *Oxidation of Metals* **50**, 139 (1998).
26. H. Nagai, *Materials Science Forum* **43**, 75 (1989).
27. F.J. Pérez, M.J. Cristobal, M.P. Hierro and F. Pedraza, *Surface and Coating Technology* **120-121**, 442 (1999).
28. A. Paúl, S. Elmrabet, L.C. Alves, M.F. Da Silva, J.C. Soares and J.A. Odriozola, *Nuclear Instruments and Methods in Physics Research* **B181**, 394 (2001).
29. F.H. Stott, G.C. Wood and J. Stringer, *Oxidation of Metals* **44**, 113 (1995).
30. B. Li and B. Gleeson, *Oxidation of Metals* **65**, 101 (2006).
31. T. Ishitsuka, Y. Inoue and H. Ogawa, *Oxidation of Metals* **61**, 125 (2004).
32. M. Ueda, Y. Oyama, K. Kawamura and T. Maruyama, *Materials at High Temperatures* **22**, 79 (2005).
33. M. Ueda, M. Nanko, K. Kawamura and T. Maruyama, *Materials at High Temperatures* **20**, 109 (2003).
34. H. Buscail, S. El Messki, F. Riffard, S. Perrier and C. Issartel, *Oxidation of Metals* **75**, 27 (2011).
35. F. Toscan, A. Galerie and, P.O. Santacreu, *Materials Science Forum* **461**, 45 (2004).
36. N. Fujita, K. Ohmura and A. Yamamoto, *Materials Science and Engineering* **A351**, 272 (2003).
37. J. Kallqvist and H.O. Andrén, *Materials Science and Engineering* **A270**, 27 (1999).
38. O. Yoo, Y.J. Oh, B.S. Lee and S.W. Nama, *Materials Science and Engineering* **A405**, 147 (2005).
39. F. Riffard, H. Buscail, E. Caudron, R. Cueff, C. Issartel and S. Perrier, *Journal of Materials Science* **37**, 3925 (2002).
40. F.J. Pérez, M.J. Cristobal, M.P. Hierro and F. Pedraza, *Surface and Coating Technology* **120-121**, 442 (1999).
41. P.Y. Hou and J. Stringer, *Journal de Physique IV* **C9**, 231 (1993).
42. D.L. Douglass, P. Nanni, C. De Asmundis and C. Bottino, *Oxidation of Metals* **28**, 309 (1987).
43. S. Nakakubo, M. Takeda and T. Onishi, *Materials Science Forum* **696**, 88 (2011).
44. T. Onishi, S. Nakakubo and M. Takeda, *Materials Transaction* **51**, 482 (2010).
45. P. Bettermann and F. Liebau, *Contributions to Mineralogy and Petrology* **53**, 25 (1975).
46. D. Fabian, C. Jäger, Th. Henning, J. Dorschner and H. Mutschke, *Astronomy and Astrophysics* **364**, 282 (2000).